

Dielectric versus Magnetic Pairing Mechanisms in High-Temperature Cuprate Superconductors Investigated Using Raman Scattering

B. P. P. Mallett,^{1,*} T. Wolf,² E. Gilioli,³ F. Licci,³ G. V. M. Williams,¹ A. B. Kaiser,¹ N. W. Ashcroft,⁴ N. Suresh,⁵ and J. L. Tallon⁵

¹MacDiarmid Institute, SCPS, Victoria University, P.O. Box 600, Wellington 6140, New Zealand

²Karlsruhe Institute of Technology, Postfach 3640, Karlsruhe 76021, Germany

³IMEM-CNR, Institute of Materials for Electronics and Magnetism, 43124 Parma, Italy

⁴Laboratory of Atomic and Solid State Physics, Cornell University, Ithaca, New York 14853-2501, USA

⁵MacDiarmid Institute, P.O. Box 31310 Lower Hutt, New Zealand

(Received 4 October 2012; revised manuscript received 16 May 2013; published 5 December 2013)

We suggest, and demonstrate, a systematic approach to the study of cuprate superconductors, namely, progressive change of ion size in order to systematically alter the interaction strength and other key parameters. $R(\text{Ba}, \text{Sr})_2\text{Cu}_3\text{O}_y$ ($R = \{\text{La}, \dots, \text{Lu}, \text{Y}\}$) is such a system where potentially obscuring structural changes are minimal. We thereby systematically alter both dielectric and magnetic properties. Dielectric fluctuation is characterized by ionic polarizability while magnetic fluctuation is characterized by exchange interactions measurable by Raman scattering. The range of transition temperatures is 70–107 K, and we find that these correlate only with the dielectric properties, a behavior which persists with external pressure. The ultimate significance may remain to be proven, but it highlights the role of dielectric screening in the cuprates and adds support to a previously proposed novel pairing mechanism involving exchange of quantized waves of electronic polarization.

DOI: 10.1103/PhysRevLett.111.237001

PACS numbers: 74.62.-c, 74.25.Ha, 74.25.nd, 74.72.Cj

The physical mechanism for electron pairing in cuprate superconductors remains uncertain. While there may be a broad consensus that it is probably magnetic in origin [1] a continuing challenge was the apparent low spectral weight of associated spin fluctuations, as measured by inelastic neutron scattering [2]. Recent studies using resonant inelastic x-ray scattering (RIXS) seem to locate the missing weight by identifying intense paramagnon excitations across the entire superconducting phase diagram [3]. However, there are major material-dependent variations in superconducting properties, as summarized in Fig. 1 (see also [4]), that remain unexplained, and any successful theory must account for these. The basic Hubbard model can account for the observed generic phase behavior as a function of interaction strength and doping [5] but not for these material-dependent systematics. The problem is exacerbated by the complex and variable structure of the cuprates where some of the behavior may be systematic while some may be attributable to disorder [6], or uncontrolled structural variation in terms of, e.g., buckling angles and apical oxygen bond lengths.

We propose an approach to resolving this impasse by developing a suite of experiments that explore the effects of external pressure and changing ion size (internal pressure) on all the key energy scales using a model system in which structural variables remain essentially unchanged. In this way the true underlying material-dependent variation might be exposed and at the same time be used to test competing theoretical models. At the very least this offers a way to systematically vary the interaction strength, a probe

which has hitherto been missing in experimental studies. We illustrate the approach in the model system $R(\text{Ba}, \text{Sr})_2\text{Cu}_3\text{O}_y$ by studying the systematic variation in the nearest-neighbor exchange interaction J as measured by Raman two-magnon scattering under changing external and internal pressure. In $R(\text{Ba}, \text{Sr})_2\text{Cu}_3\text{O}_y$ the change in buckling angle is less than 2° for a given doping [7,8] and

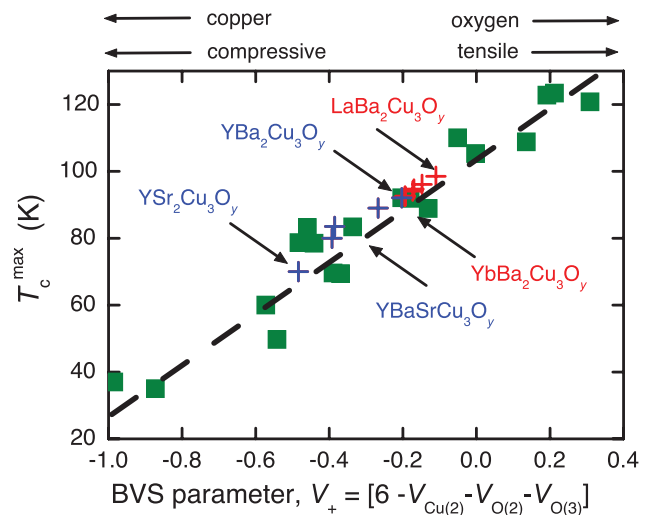


FIG. 1 (color). T_c^{\max} , plotted as a function of the bond valence sum parameter $V_+ = 6 - V_{\text{Cu}(2)} - V_{\text{O}(2)} - V_{\text{O}(3)}$. Green squares: as previously reported [12]; red crosses: $R\text{Ba}_2\text{Cu}_3\text{O}_y$ ($R = \text{La}, \text{Nd}, \text{Sm}, \text{Gd}, \text{Dy}, \text{and Yb}$); blue crosses: $\text{YBa}_{2-x}\text{Sr}_x\text{Cu}_3\text{O}_y$ ($x = 0, 0.5, 1.0, 1.25, \text{and } 2$).

disorder is essentially absent in the end members. Even for $\text{YBaSrCu}_3\text{O}_y$, we find no suppression of superfluid density as measured by muon spin relaxation [9] which might arise from disorder. Moreover, the ion-size-dependent strain tensor for this system reduces to a nearly pure dilatation with almost no tetragonal or orthorhombic distortion; see Supplemental Material [10].

We find that internal and external pressures have identical effects on J but opposite effects on T_c^{max} . Though T_c^{max} fails to correlate with J , it does correlate with the dielectric properties as described by the refractivity sum $\sum_i n_i \alpha_i$, where n_i are the ion densities and α_i their polarizabilities, thus highlighting the key role of dielectric screening. While this work leaves some open questions, the correlations elucidated do warrant further study. At the least, it does illustrate a necessary and overdue systematic approach to the study of cuprate physics which hitherto has largely been confined to comparative studies of $\text{YBa}_2\text{Cu}_3\text{O}_y$, $\text{Bi}_2\text{Sr}_2\text{CaCu}_2\text{O}_{8+\delta}$, and $(\text{La, Sr})_2\text{CuO}_4$ —widely differing systems. The approach can easily be extended to study systematic changes in electronic structure and low-energy excitations in the cuprates.

We are motivated by a central paradox of cuprate physics: external pressure increases T_c^{max} [11], whereas internal pressure, as induced by isovalent ion substitution, decreases T_c^{max} [12,13]. Figure 1 shows T_c^{max} plotted against the composite bond valence sum parameter, $V_+ = 6 - V_{\text{Cu}(2)} - V_{\text{O}(2)} - V_{\text{O}(3)}$, taken from Ref. [12] (green squares). Here $V_{\text{Cu}(2)}$, $V_{\text{O}(2)}$, and $V_{\text{O}(3)}$ are the planar copper and oxygen bond valence sum parameters and the plot reveals a remarkable correlation of T_c^{max} across single-, two-, and three-layer cuprates. We may write $V_+ = (2 - V_{\text{O}(2)}) + (2 - V_{\text{O}(3)}) - (V_{\text{Cu}(2)} - 2)$ and hence V_+ is a measure of doped charge distribution between the Cu and O orbitals [14] but is also a measure of in-plane stress [15], as noted at the top of the figure. Evidently stretching the CuO_2 plane increases T_c^{max} . However, V_+ is a compound measure and also reflects physical displacement of the apical oxygen away from the Cu atoms.

Crucially, this plot reveals that all cuprates follow a systematic behavior. There are no anomalous outliers. It is common to regard $\text{La}_{2-x}\text{Sr}_x\text{CuO}_4$ as anomalous because of its propensity for disorder. But the leftmost data point in Fig. 1 shows that it is entirely consistent with the other cuprates. It remains then to determine just what this V_+ parameter encapsulates so systematically.

To this plot we add new data for the superconductors $R\text{Ba}_{2-x}\text{Sr}_x\text{Cu}_3\text{O}_y$, as R is varied with $x = 0$ (red crosses) and, in the case of $R = \text{Y}$, $x = 0, 0.5, 1, 1.25,$ and 2 (blue crosses). We use the structural refinements of Guillaume *et al.* [7], Licci *et al.* [8], and Gilioli *et al.* [16] and calculate V_+ in the same way as previously [12]. Notably, the global correlation is also preserved across this model system, reflecting the progressive compression of the lattice as ion size decreases and the effective internal

pressure increases. Figure 1 thus summarizes a general feature of the cuprates, namely, that internal pressure decreases T_c^{max} while external pressure increases T_c^{max} [11]. What then is the salient difference between internal and external pressure on T_c^{max} ?

The magnitude of T_c^{max} will be set in part by the energy scale, $\hbar\omega_B$, of the pairing boson and also by $N(E)$, the electronic density of states (DOS). In the underdoped regime the DOS is progressively depleted by the opening of the pseudogap, whereas the overdoped DOS is enhanced by the proximity of the van Hove singularity. Here we focus on $\hbar\omega_B$, which in many magnetic pairing models is governed to leading order by J [1,3,17]; see Ref. [10] for details. In the one-band Hubbard model, $J = -4t^2/U$, where t is the nearest-neighbor hopping integral and U is the on-site Coulomb repulsion energy. Our question then is, does T_c^{max} correlate with J ?

We measured J in single crystals of deoxygenated $R\text{Ba}_2\text{Cu}_3\text{O}_6$ (R -123) using B_{1g} Raman scattering where the two-magnon peak occurs at frequency $\omega_{\text{max}} = 3.2J/\hbar$ [18]. We choose deoxygenated R -123 because the undoped state is the only truly reproducible doping level across the R series and, moreover, the two-magnon peak is not easy to resolve at optimal doping. Though J is doping dependent, we fully expect that it will retain the same systematic variation with ion size reported below for all doping levels. The normalized raw data are shown in the inset of Fig. 2. As the R ion size decreases, the B_{1g} two-magnon peak shifts to higher energy as expected due to the increased overlap between Cu $3d$ and O $2p$ orbitals.

The relative shift in effective internal pressure ΔP_{eff} may be estimated from the change in volume ΔV using $\Delta P_{\text{eff}} = -B \cdot \Delta V/V_0$, where $B = 78.1$ GPa is the bulk modulus for deoxygenated $\text{YBa}_2\text{Cu}_3\text{O}_6$ [19] and

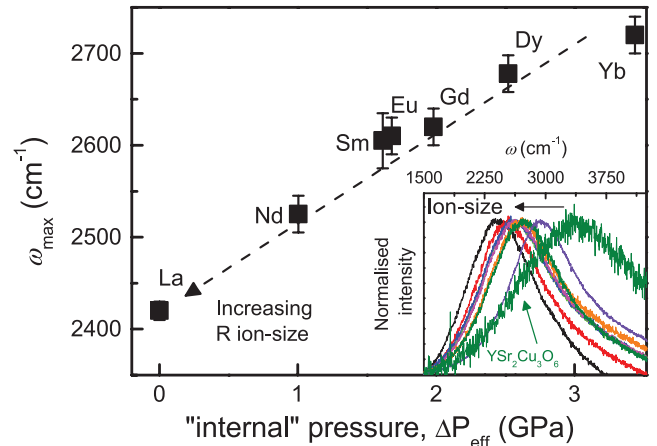


FIG. 2 (color). The B_{1g} Raman two-magnon peak frequency ω_{max} for each $R\text{Ba}_2\text{Cu}_3\text{O}_6$ (R -123) sample plotted against the effective internal pressure using $\Delta P_{\text{eff}} = -B \cdot \Delta V/V_0$, where $B = 78.1$ GPa is the bulk modulus [19] and $\Delta V = V - V_0$ is referenced to La-123. The inset shows normalized Raman spectra for R -123 single crystals and for polycrystalline $\text{YSr}_2\text{Cu}_3\text{O}_6$.

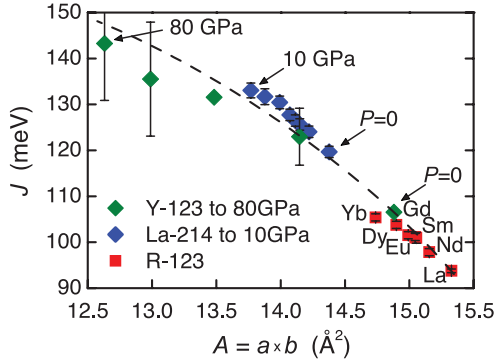


FIG. 3 (color). The unit-cell basal plane area (A) dependence of J determined from two-magnon scattering on $RBa_2Cu_3O_6$ (red squares) where “internal pressure” is the implicit variable. The effect of external pressure [20] is also shown for La_2CuO_4 (0 to 10 GPa, blue diamonds) and $YBa_2Cu_3O_{6.2}$ to 80 GPa [21] (green diamonds).

$\Delta V = V - V_0$ is referenced to La-123. We plot ω_{\max} versus ΔP_{eff} in Fig. 2. Further, the dependence of J on basal area A is plotted in Fig. 3. To this we also show in Fig. 3 the effect of external pressure on J in La_2CuO_4 [20] (blue diamonds) ranging up to 10 GPa, as annotated, and for $YBa_2Cu_3O_{6.2}$ under external pressure up to 80 GPa [21] (green diamonds). Bearing in mind the nonlinearity that must occur on approaching 80 GPa, the dependence of J on A is similar across the entire range, irrespective of whether the pressure is *internal* or *external* in origin. We expect this uniform dependence to be preserved at optimal doping. This is our first main result and it contrasts the opposing effects of internal and external pressure on T_c^{\max} .

We now plot in Fig. 4(a) T_c^{\max} versus J for the R -123 single-crystal series (red squares) using $T_c^{\max} = 98.5$ K for La-123 [22] and $T_c^{\max} = 96$ K for Nd-123 [23] since these are the highest reported values of T_c^{\max} in these cuprates (where R occupation of the Ba site is minimized). Interestingly, T_c^{\max} anticorrelates with J .

To move to yet higher J values, we repeated the Raman measurements on a c -axis aligned thin film of $YBa_{1.5}Sr_{0.5}Cu_3O_6$ and on individual grains of polycrystalline $YSr_2Cu_3O_6$ prepared under high-pressure or high-temperature synthesis [16] [blue diamonds in Fig. 4(a)]. The anticorrelation between T_c^{\max} and J is preserved, but now out to a more than 60% increase in the value of J . This is a very large increase and it is perhaps surprising that it is not reflected in the value of T_c^{\max} if magnetic interactions alone set the energy scale for pairing.

To this plot we add data showing the effect of external pressure on T_c^{\max} and J in $YBa_2Cu_3O_7$ (green squares, for 0, 1.7, 4.5, 14.5, and 16.8 GPa). The shift in J with pressure is taken from Fig. 3 and the values of T_c^{\max} at elevated pressures are from Refs [24,25]; see Ref. [10]. We note that the effects of external and internal pressure are orthogonal, highlighting the fact that the observed shifts in T_c^{\max} simply do not correlate with J . This is our second main result.

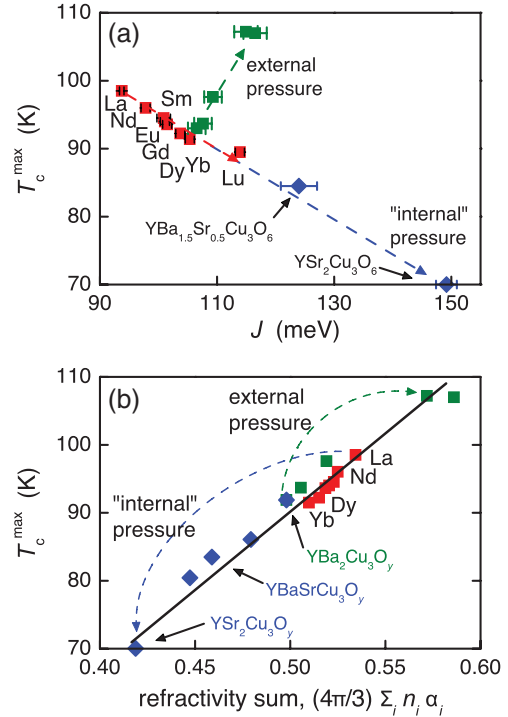


FIG. 4 (color). (a) T_c^{\max} plotted versus J for single crystals of $RBa_2Cu_3O_6$ (red squares) and for $YBa_{2-x}Sr_xCu_3O_6$ (blue diamonds) with $x = 0.5$ and 2.0 . T_c^{\max} anticorrelates with J where “internal pressure” (blue trajectory) is the implicit variable. The green squares show that T_c^{\max} versus J under external pressure (green trajectory) is effectively orthogonal to the behavior for internal pressure. (b) T_c^{\max} plotted against the polarizability sum $(4\pi/3)\sum_i n_i \alpha_i$ for $RBa_2Cu_3O_y$ (red squares, $R = \text{La, Nd, Sm, Eu, Gd, Dy, Yb}$) and $YBa_{2-x}Sr_xCu_3O_y$ (blue diamonds, $x = 0, 0.5, 1.0, 1.25,$ and 2) which summarize the effects of internal pressure. The green squares show T_c^{\max} versus $(4\pi/3)\sum_i n_i \alpha_i$ for $YBa_2Cu_3O_y$ under external pressure, revealing a correlation which remains consistent with that for internal pressure.

These results differ from Ofer *et al.* [26] who reported correlations between T_c^{\max} and the Néel temperature T_N in $(La_{1-x}Ca_x)(Ba_{1.75-x}La_{0.25+x})Cu_3O_y$. However, the effects they report are quite small compared with ours. Moreover, since T_N is not directly related to J their analysis required a model to estimate the exchange anisotropy and thereby convert T_N to J . We also note that this complex system has large nuclear quadrupole resonance linewidths reflecting a high degree of disorder. In our view the present study is more direct and reliable in its implications considering we have an ideal model system with constant buckling angle, an essentially pure dilatation strain tensor and relatively disorder free. There may be some other systematic internal structural change which underlies our correlations, but it is not yet evident.

B_{1g} scattering only probes nearest-neighbor magnetic interactions [27] while recent RIXS studies [28] reveal the presence of extended interactions involving next-nearest- and next-next-nearest-neighbor hopping integrals,

t' and t'' [29]. The additional extended exchange interaction is only about half the magnitude of the changes that we have imposed by ion-size variation. It is conceivable that inclusion of extended interactions might reverse the systematics reported here; however, in our view variations in t' and t'' will have a stronger influence via the DOS by distorting the Fermi surface and shifting the van Hove singularity. RIXS studies of ion-size effects on t' and t'' using our model system would settle this important question.

The contradictory behavior shown in Fig. 4(a) contrasts the uniform simplicity of Fig. 1 and suggests that some new element is needed to understand ion-size systematics. One arena where ion size plays a key role is in the dielectric properties, where the ionic polarizability generally varies as the cube of the ion size [30].

The isolated CuO_2 planar array is electrostatically uncompensated and as such cannot constitute a thermodynamic system. It is necessary to include the compensating charges lying outside of the CuO_2 plane in any thermodynamic treatment and these will also mediate electron-electron interactions within the plane. These charges reside on ions that are notably polarizable, resulting in the high dielectric constants observed in the cuprates [31] and which will screen electronic interactions in the CuO_2 layers via incoherent fluctuations in polarization. Additionally, there are *coherent* excitations in such a medium giving rise to quantized bosonic polarization waves which can mediate *d*-wave pairing with a very large pre-factor energy scale [10,32].

In an early treatment of dielectric properties Goldhammer [33] showed for sufficiently symmetric systems that the dielectric constant contains an enhancement factor $[1 - (4\pi/3)\sum_i n_i \alpha_i]^{-1}$ leading in principle to “polarization catastrophe” when $(4\pi/3)\sum_i n_i \alpha_i \rightarrow 1$. (The factor $(4\pi/3)$ is dependent on structure, the dielectric constant more generally being replaced by a dielectric matrix, and in a fuller treatment the enhancement factor is replaced by frequency- and momentum-dependent terms [32].)

We focus first on the contributions from the noncuprate layers, and in Fig. 4(b) we plot T_c^{max} versus $(4\pi/3)\sum_i n_i \alpha_i$ for $R(\text{Ba}, \text{Sr})_2\text{Cu}_3\text{O}_y$, where the sum is over R , Ba, Sr, and the apical O(4) oxygens. Red squares summarize the effects of changing R and blue diamonds the effects of replacing Ba by Sr. These are the internal pressure effects and the correlation is excellent. The polarizabilities are taken from Shannon [30]. If this correlation is to be meaningful, it must resolve the paradox of the opposing effects of internal and external pressure. Qualitatively this seems possible because increasing ion size (decreasing internal pressure) increases the polarizability while increasing external pressure enhances the densities n_i , in both cases increasing the dielectric enhancement factor. To test this we also plot T_c^{max} versus $(4\pi/3)\sum_i n_i \alpha_i$ for $\text{YBa}_2\text{Cu}_3\text{O}_7$

at 1 atm and 1.7, 4.5, 14.5, and 16.8 GPa (green squares) where we assume to first order that only the n_i , and not the α_i , alter under pressure. For more details, see Ref. [10]. The correlation with polarizability is now preserved over a range of T_c^{max} from 70 to 107 K, including both internal and external pressure. This is our third main result and it partly explains the correlation with V_+ shown in Fig. 1. The additional role of the apical oxygen bond length (which also contributes to the value of V_+) has yet to be clarified, but it may play a supplementary role in controlling the large polarizability of the Zhang-Rice singlet [34] as distinct from controlling its stability as discussed by Ohta *et al.* [4].

As shown in [10], inclusion of the refractivities from the CuO_2 layers preserves the correlation with T_c^{max} but adds a further 0.4 to the refractivity sum bringing these systems close to polarization catastrophe. In practice this can implicate an insulator-to-metal transition or charge ordering, both of which are evident in the cuprates.

What may we conclude? These correlations might hint at a dielectric rather than magnetic pairing mechanism, but it remains to be shown that the effects described here are not a proxy for some other structural systematics. And dielectric effects impact on magnetic interactions: a highly polarizable medium could merely be effective in screening long-range magnetic interactions [35], or the on-site Hubbard U [36], by means of local *incoherent* fluctuations. On the other hand, *coherent* fluctuations of this medium, quantized waves of polarization, do mediate pairing on a large energy scale [32] and might in fact be the elusive exchange boson. Both of these distinct scenarios can be tested. Certainly the correlations reported here warrant deeper investigation.

Finally, based on our observed correlation and an inferred polarizability of $\alpha_{\text{Ra}} = 8.3 \text{ \AA}^3$ for the radium ion [10], we predict $T_c^{\text{max}} \approx 109 \pm 2 \text{ K}$ for $\text{YRa}_2\text{Cu}_3\text{O}_y$ and $117 \pm 2 \text{ K}$ for $\text{LaRa}_2\text{Cu}_3\text{O}_y$. A more amenable test is that T_c^{max} for $\text{Bi}_2\text{Sr}_{1.6}\text{La}_{0.4}\text{CuO}_6$ will be raised by substituting the more polarizable Ba for Sr, despite the introduction of additional disorder.

In summary, we describe a strategy that utilizes ion-size and external-pressure effects to measure how systematic changes in U , t , t' , and t'' relate to superconductivity in the cuprates. We apply this strategy to show that internal and external pressures have identical effects on the characteristic energy scale $J = -4t^2/U$ but opposite effects on T_c^{max} , so that the latter does not correlate with the former. These results suggest that longer-range interactions play a significant role in defining the systematics of T_c^{max} in relation to structure and this role is governed by screening arising from the total system of core electrons, including the non- CuO_2 layers. This is supported by our finding that T_c^{max} correlates exceptionally well with the refractivity sum, for both internal and external pressures. We suggest that a novel pairing mechanism involving coherent

collective excitations associated with the ionic polarizabilities should be further explored.

This work is funded by the Marsden Fund (G. V. M. W., N. S., J. L. T.), the MacDiarmid Institute (B. P. P. M., J. L. T.), and the National Science Foundation, DMR-0907425 (N. W. A.).

*Corresponding author.

benjamin.mallett@unifr.ch

- [1] D. J. Scalapino, *Rev. Mod. Phys.* **84**, 1383 (2012).
- [2] E. G. Maksimov, M. L. Kulić, and O. V. Dolgov, *Adv. Condens. Matter Phys.* **2010**, 423725 (2010).
- [3] M. Le Tacon *et al.*, *Nat. Phys.* **7**, 725 (2011).
- [4] Y. Ohta, T. Tohyama, and S. Maekawa, *Phys. Rev. B* **43**, 2968 (1991).
- [5] E. Gull, O. Parcollet, and A. J. Millis, *Phys. Rev. Lett.* **110**, 216405 (2013).
- [6] H. Eisaki, N. Kaneko, D. Feng, A. Damascelli, P. Mang, K. Shen, Z.-X. Shen, and M. Greven, *Phys. Rev. B* **69**, 064512 (2004).
- [7] M. Guillaume, P. Allenspach, W. Henggeler, J. Mesot, B. Roessli, U. Staub, P. Fischer, A. Furrer, and V. Trounov, *J. Phys. Condens. Matter* **6**, 7963 (1994).
- [8] F. Licci, A. Gauzzi, M. Marezio, G. P. Radaelli, R. Masini, and C. Chailout-Bougerol, *Phys. Rev. B* **58**, 15208 (1998).
- [9] B. P. P. Mallett, Ph.D. thesis, Victoria University of Wellington, (2013), [arXiv:1310.3055](https://arxiv.org/abs/1310.3055).
- [10] See Supplemental Material at <http://link.aps.org/supplemental/10.1103/PhysRevLett.111.237001> for further details.
- [11] J. Schilling, in *Handbook of High-Temperature Superconductivity*, edited by J. Schrieffer and J. Brooks (Springer, New York, 2007), pp. 427–462.
- [12] J. L. Tallon, *Physica (Amsterdam) C* **168**, 85 (1990).
- [13] M. Marezio, E. Gilioli, P. Radaelli, A. Gauzzi, and F. Licci, *Physica (Amsterdam) C* **341–348**, 375 (2000).
- [14] I. Brown and D. Altermatt, *Acta Crystallogr. Sect. B* **41**, 244 (1985).
- [15] I. Brown, *J. Solid State Chem.* **82**, 122 (1989).
- [16] E. Gilioli, P. Radaelli, A. Gauzzi, F. Licci, and M. Marezio, *Physica (Amsterdam) C* **341–348**, 605 (2000).
- [17] H.-Y. Kee, S. A. Kivelson, and G. Aeppli, *Phys. Rev. Lett.* **88**, 257002 (2002).
- [18] A. V. Chubukov and D. M. Frenkel, *Phys. Rev. B* **52**, 9760 (1995).
- [19] K. Suenaga and G. Oomi, *J. Phys. Soc. Jpn.* **60**, 1189 (1991).
- [20] M. C. Aronson, S. B. Dierker, B. S. Dennis, S. W. Cheong, and Z. Fisk, *Phys. Rev. B* **44**, 4657 (1991).
- [21] A. Maksimov and I. Tartakovskii, *J. Supercond.* **7**, 439 (1994).
- [22] T. Lindemer, B. Chakoumakos, E. Specht, R. Williams, and Y. Chen, *Physica (Amsterdam) C* **231**, 80 (1994).
- [23] B. W. Veal, A. P. Paulikas, J. W. Downey, H. Claus, K. Vandervoort, G. Tomlins, H. Shi, M. Jensen, and L. Morss, *Physica (Amsterdam) C* **162–164**, 97 (1989).
- [24] M. McElfresh, M. Maple, K. Yang, and Z. Fisk, *Appl. Phys. A* **45**, 365 (1988).
- [25] S. Sadewasser, J. S. Schilling, A. P. Paulikas, and B. W. Veal, *Phys. Rev. B* **61**, 741 (2000).
- [26] R. Ofer, G. Bazalitsky, A. Kanigel, A. Keren, A. Auerbach, J. S. Lord, and A. Amato, *Phys. Rev. B* **74**, 220508 (2006).
- [27] R. R. P. Singh, P. A. Fleury, K. B. Lyons, and P. E. Sulewski, *Phys. Rev. Lett.* **62**, 2736 (1989).
- [28] M. Guarise *et al.*, *Phys. Rev. Lett.* **105**, 157006 (2010).
- [29] E. Pavarini, I. Dasgupta, T. Saha-Dasgupta, O. Jepsen, and O. K. Andersen, *Phys. Rev. Lett.* **87**, 047003 (2001).
- [30] R. Shannon, *J. Appl. Phys.* **73**, 348 (1993).
- [31] D. Reagor, E. Ahrens, S. W. Cheong, A. Migliori, and Z. Fisk, *Phys. Rev. Lett.* **62**, 2048 (1989).
- [32] G. S. Atwal and N. W. Ashcroft, *Phys. Rev. B* **70**, 104513 (2004); N. W. Ashcroft, in *Novel Superconductivity* edited by S. A. Wolf and V. Kresin (Plenum, New York, 1987), pp. 301–308.
- [33] D. Goldhammer, *Mathematisch-physikalische Schriften für Ingenieure und Studierende*, edited by E. Jahnke (B. G. Teubner, Leipzig, Germany, 1913), Nr. 16.
- [34] F. C. Zhang and T. M. Rice, *Phys. Rev. B* **37**, 3759 (1988).
- [35] S. Raghu, R. Thomale, and T. H. Geballe, *Phys. Rev. B* **86**, 094506 (2012).
- [36] J. van den Brink, M. B. J. Meinders, J. Lorenzana, R. Eder, and G. A. Sawatzky, *Phys. Rev. Lett.* **75**, 4658 (1995).